A theoretical study of the staggered and eclipsed forms of the dinuclear complex MnRe(CO)(10)

A theoretical study of the staggered and eclipsed forms of the dinuclear complex MnRe(CO)10

Michael H. Palmer, Philip J. Camp, Chakree Tanjaroon, Kristen S. Keck, and Stephen G. Kukolich

Citation: J. Chem. Phys. **121**, 7187 (2004); doi: 10.1063/1.1790991
View online: http://dx.doi.org/10.1063/1.1790991
View Table of Contents: http://jcp.aip.org/resource/1/JCPSA6/v121/i15
Published by the AIP Publishing LLC.

A theoretical study of the staggered and eclipsed forms of the dinuclear complex $MnRe(CO)_{10}$

Michael H. Palmer and Philip J. Camp
School of Chemistry, University of Edinburgh, West Mains Road, Edinburgh EH9 3JJ, United Kingdom

Chakree Tanjaroon, Kristen S. Keck, and Stephen G. Kukolich
Department of Chemistry, University of Arizona, Tucson, Arizona 85721

(Received 18 June 2004; accepted 19 July 2004)

Two possible conformers of the dinuclear complex $MnRe(CO)_{10}$, each of C_{4v} symmetry, with eclipsed and staggered conformations, have been analyzed theoretically. Using both the B3LYP and BP86 density functionals we find that the staggered form is lower in energy. A determination of the B3LYP potential energy surface as a function of the Mn-Re distance is presented for both conformers. The computed bond lengths, bond angles, and rotational constant for the staggered conformation compare favorably with the results from microwave experiments. The harmonic frequencies for the staggered structure have been determined using several basis sets, with both analytical and finite difference methods. These unscaled vibrational frequencies, together with their intensities for both infrared and Raman activity, are used to assign the three most intense experimental IR and Raman bands, and in particular, the ν_{CO} region. The lowest A_2 vibration was calculated to occur at 41 cm^{-1} in the staggered conformer; this frequency becomes imaginary in the (saddle point) eclipsed form. Several fundamentals remain to be observed experimentally. © *2004 American Institute of Physics.* [DOI: 10.1063/1.1790991]

I. INTRODUCTION

Recently we reported[1] the microwave (MW) rotational spectrum of the $MnRe(CO)_{10}$ complex, a molecule with C_{4v} symmetry, together with a series of *ab initio* calculations using large Gaussian orbital bases (GTOs). The calculations both assisted the spectral assignment and gave important information concerning the electronic structure of the molecule. The MW spectrum exhibits a prolate symmetric-top rotational spectrum with large hyperfine structure, due to both Re and Mn nuclear quadrupole interactions. However, because the rotational constants and rotational spectrum for a specific set of structural parameters do not differ between the staggered and eclipsed C_{4v} conformers, as shown in Fig. 1 the study was incomplete, and we now report a more detailed theoretical study which includes both conformations. In addition, the effects of conformational (torsional and vibrational) averaging in the experimental quadrupole coupling constant results are considered theoretically. The infrared and Raman spectra of this compound have been widely reported, and the present study offers a detailed discussion of the band assignments utilizing harmonic frequencies.

II. THEORETICAL METHODS

Calculations were performed using the GAMESS-UK suite of programs.[1–3] All-electron basis sets for both Mn and Re are necessary if the quadrupolar interactions are to be taken fully into account, and the present study closely follows our previous work reported in Ref. 1. More than one basis set was used for reasons described below. The main study used an uncontracted $14s10p7d$ Mn basis set, contracted $[s/p/d/f]$ to $[3,1^{11}/3,1^{7}/4,1^{4}]$, while that for Re was $25s19p15d10f$ contracted to $[8,3,2,1^{12}/7,1^{12}/6,2,1^{7}/7,3]$. Here the superscript shows the number of single functions. The C and O $(11s7p2d)$ functions were also largely uncontracted, to either $[5,1^{6}/3,1^{4}/1^{2}]$ or $[6,1^{5}/4,1^{3}/1^{2}]$, and hence are similar to TZ2P bases. These bases generate a total of either 874 or 784 Cartesian GTOs $(6d,10f)$, respectively, where the former allows a little more flexibility in the C and O bases. A 681 GTO calculation of TZ2P quality, including two *d*-type polarization functions on C and O, was the largest possible for both infrared and Raman frequency and intensity determination. The *d*- and *f*-orbital sets were used as the spherical harmonic $(5d,7f)$ rather than the Cartesian choice, because of problems with implicit *s* and *p* functions in the latter leading to linear dependence. These were indicated in the Tables of Ref. 1 as 784→724, 874→814, etc. The density functional theory (DFT) methodology used follows that from our previous study, i.e., B3LYP and BP86 functionals.

The large bases used in this study caused difficulty in obtaining convergence to the lowest energy state, especially when starting far from the equilibrium structure. Extensive level shifting was necessary, and it was often advantageous to avoid usage of the DIIS (direct inversion of iterated space) extrapolation technique. A procedure which was useful in the present work, and the previous study,[1] was to initially calculate the wave function of the unrestricted Hartree-Fock (UHF) triplet state at the required Mn-Re distance. This procedure is generally quite simple to carry out. The highest occupied molecular orbital (HOMO) and HOMO-1 [MOs (MOs—molecular orbitals) 121 and 120] are heavily local-

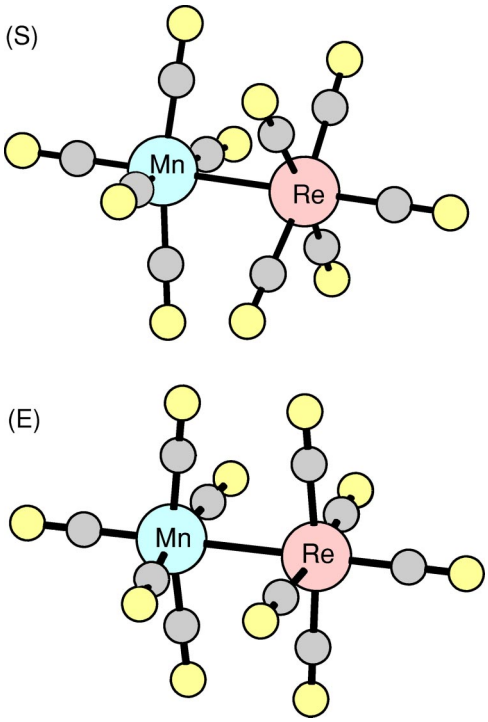

FIG. 1. Structures for the staggered (*S*) and eclipsed (*E*) conformers of the Mn $Re(CO)_{10}$ dinuclear complex. The staggered form has the lowest calculated energy and calculated Mn-Re bond length which is in best agreement with the experimental (MW) value.

ized on the Re and Mn atoms, respectively, and restoring this wave function into the desired singlet state gave a good starting wave function.

Harmonic frequencies were determined by both analytical (smaller bases) and finite difference (FD) procedures (for the largest 784 basis set calculations), using the B3LYP methodology throughout. The FD method used three-point differences (i.e., equilibrium position with positive and negative coordinate FDs of ± 0.0005 a.u.), and a wave function convergence of 10^{-7}. Under these conditions, the degenerate pairs of "*E*" vibrations were $\approx \pm 0.0001$ cm^{-1}. Two-point calculations and a poorer level (10^{-6}) of wave function convergence gave *E* vibrations with frequencies differing by ~ 0.1 cm^{-1}, which were still recognizable as *E* type.

III. RESULTS AND DISCUSSION

A. Structural features

Some equilibrium structural properties computed using the 874 basis set are summarized in Table I. With this basis set, however, the size of the computations precluded a systematic survey of the potential-energy surface. The BP86 functional gives marginally shorter Mn-Re bond lengths for the staggered and eclipsed conformations of 3.0772 Å and 3.1401 Å, respectively, compared to the corresponding B3LYP values of 3.0864 Å and 3.2235 Å. The MW value reported in Ref. 1 is 2.99 Å, whereas x-ray determinations lead to equilibrium values of 2.96 Å (Ref. 4) and 2.909(1) Å

TABLE I. Summary of equilibrium properties of Mn $Re(CO)_{10}$ computed using the 874 basis set and the B3LYP and BP86 functionals. Bond lengths and angles are given in angstroms and degrees, respectively.

	B3LYP		BP86	
Methodology	Staggered	Eclipsed	Staggered	Eclipsed
Total energy/a.u.	−18 066.1581	−18 066.1520	−18 067.6015	−18 067.5950
DipoleMoment/D	1.3378	1.4112	1.5813	1.7377
Rotation constant (*B*/MHz)	188.7688	178.4003	186.7081	181.9929
Mn centered				
Mn Re	3.0864	3.2235	3.0772	3.1401
MnC_{ax}	1.8188	1.8231	1.8064	1.8126
$C_{ax}O_{ax}$	1.1423	1.1447	1.1576	1.1585
MnC_{eq}	1.8650	1.8642	1.8511	1.8481
$C_{eq}O_{eq}$	1.1416	1.1405	1.1560	1.1562
$MnC_{eq}O_{eq}$	178.39	176.59	177.49	175.33
Re MnC_{eq}	85.16	86.03	85.42	86.56
$C_{ax}MnC_{eq}$	94.84	93.97	94.58	93.44
cis-$C_{eq}MnC_{eq}$	89.59	89.73	89.64	89.79
trans-$C_{eq}MnC_{eq}$	170.33	172.06	170.84	173.11
$C_{ax}MnC_{eq}O_{eq}$	0.0	0.0	0.0	0.0
Re $MnC_{eq}O_{eq}$	180.0	180.0	180.0	180.0
Re centered				
Re C_{ax}	2.0034	1.9942	1.9881	1.9704
$C_{ax}O_{ax}$	1.1414	1.1412	1.1558	1.1549
Re C_{eq}	2.0688	2.0676	2.0580	2.0589
$C_{eq}O_{eq}$	1.1365	1.1366	1.1500	1.1503
Re $C_{eq}O_{eq}$	179.40	178.48	178.61	178.44
Mn Re C_{eq}	87.08	87.83	87.50	88.41
C_{ax} Re C_{eq}	92.92	92.17	92.50	91.59
cis-C_{eq} Re C_{eq}	89.85	89.92	89.89	89.96
trans-C_{eq} Re C_{eq}	174.16	175.66	175.00	176.83
C_{ax} Re $C_{eq}O_{eq}$	0.0	180.0	0.0	0.0
Mn Re $C_{eq}O_{eq}$	180.0	0.0	180.0	180.0

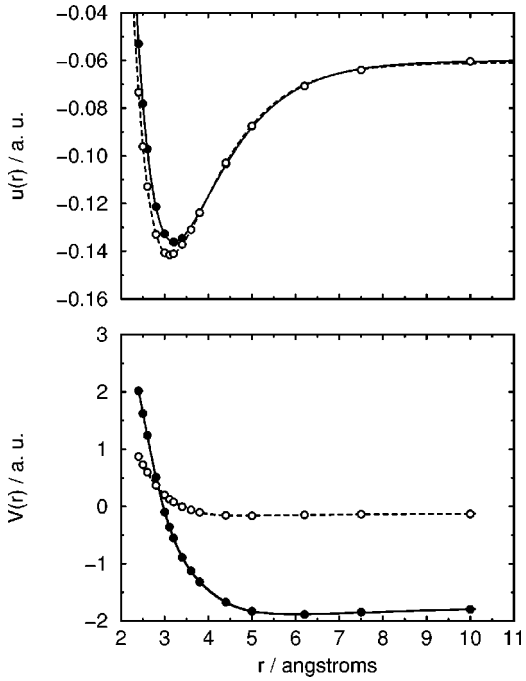

FIG. 2. The variation of the potential energies and electric field gradients of $Mn\,Re(CO)_{10}$ with the Mn-Re separation, r: (top) the potential energies in the staggered (open circles and dashed line) and eclipsed (filled circles and solid line) conformers; (bottom) the electric field gradients (EFGs) in the staggered conformer at the Mn center (open circles and dashed line) and at the Re center (filled circles and solid line). In both graphs the points are the DFT results and the lines are fits (see text).

(Ref. 5) and an identification of the point group as D_{4d}.[5] These experimental values are within the range of some other Mn-Re dinuclear complexes (2.817-2.96 Å)[6–8] and similar to the sum of the covalent radii (Mn: 1.39 Å, Re: 1.53 Å, Sum: 2.92 Å).[9] Despite the small variation in these experimental values, the theoretical Mn-Re bond length for the *staggered* conformation agrees best with observation.

B. The potential energy surface

In Fig. 2 we show the potential energy as a function of Mn-Re distance obtained using the same 784→724 basis as in Ref. 1, using the B3LYP functional. Clearly, the staggered conformation is more stable than the eclipsed form, although this distinction becomes blurred for Mn-Re distances above about 5 Å. In these computations, the electronic state was held overall as the $^1A_1$ state. At dissociation, the true electronic state would be $^2A_1+{}^2A_1$ for the two $X(CO)_5$ radical moieties (X=Mn and Re). The results were fitted using the Morse potential given by

$$u(r)=u_0+D_e\{1-\exp[-\beta(r-r_e)]\}^2, \tag{1}$$

where u_0 is an (arbitrary) offset. The fit parameters and estimated uncertainties are reported in Table II. The fits are also included in Fig. 2, which shows that the Morse potential gives a satisfactory description of the DFT results. Mass spectrometric studies of $Mn\,Re(CO)_{10}$ indicated that the dissociation energy of the Mn-Re bond is 210 kJ mol^{-1} (Ref. 4). This is in excellent agreement with our fitted value of $D_e=212\pm1$ kJ mol^{-1} for the staggered conformation, but clearly different from that for the eclipsed conformation ($D_e=199\pm1$ kJ mol^{-1}). The dissociation energy (given by D_e) of the eclipsed conformer is about 6% smaller than that of the staggered conformer, reflecting the slightly higher stability of the staggered conformer. The fitted equilibrium bond lengths—given by r_e in Table II—are in good agreement with the large-basis set results given in Table I. For both the staggered and eclipsed conformers the deviations are only about 1% from the averages of the B3LYP and BP86 results given in Table I.

TABLE II. Fitted Morse-potential parameters from the B3LYP results using the 784 basis set.

Conformer	u_0 (a.u.)	D_e (a.u.)	β (Å^{-1})	r_e (Å)
Staggered	−0.1416(1)	0.0807(3)	0.913(4)	3.113(3)
Eclipsed	−0.1360(1)	0.0759(3)	0.886(4)	3.209(3)

C. Intramolecular torsional potential

The potential energy as a function of the C_{eq}-Mn-Re-C_{eq} dihedral angle ϕ is shown in Fig. 3. The results are shown relative to the equilibrium staggered conformation ($\phi=\pi/4$ radians). The energy is shown in units of kelvin (K) to facilitate a discussion of thermal averages below. Included in Fig. 3 is a Fourier-series fit of the form

$$E(\phi)=\sum_{n=0} E_{4n}\cos(4n\phi) \tag{2}$$

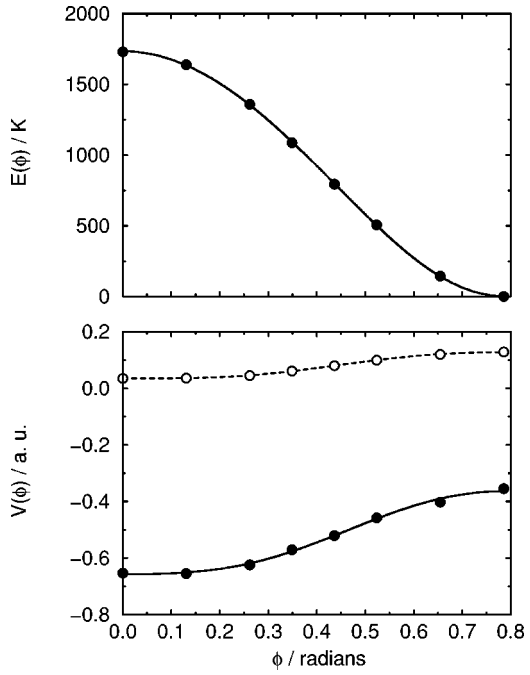

FIG. 3. The variation of the potential energy and electric field gradients of $Mn\,Re(CO)_{10}$ with the C-Mn-Re-C dihedral angle ϕ: (top) the potential energy, (bottom) the electric field gradients (EFGs) at the Mn center (open circles and dashed line) and at the Re center (filled circles and solid line). In both graphs the points are the DFT results and the lines are fits (see text).

TABLE III. Fit parameters for the torsional energy [Eq. (2)] and the electric field gradients [Eq. (5)] of Mn and Re, as functions of the dihedral angle ϕ in Mn $Re(CO)_{10}$.

		V_{4n}/a.u.	
n	E_{4n}/K	Mn center	Re center
0	908(2)	0.0761(3)	−0.530(3)
1	861(3)	−0.0491(4)	−0.150(5)
2	−40(3)	0.0056(4)	0.020(4)
3	4(3)	0.0023(4)	0.004(4)

with terms up to $n=4$. The fit parameters and the associated statistical uncertainties are reported in Table III; the barrier to internal rotation is $E(0)-E(\pi/4)=2E_0+2E_2=1736$ K, 14.4 kJ mol^{-1}.

D. Quadrupole coupling

For the equilibrium structures determined in this work, the BP86 functional with the 874 basis set gave values of the quadrupole coupling constants which are very similar to those obtained in our previous study.[1] For the ^{187}Re quadrupole coupling constant we obtain $\chi_{aa}=327.60$ MHz (eclipsed) and $\chi_{aa}=310.11$ MHz (staggered) to be compared with the experimental value of $\chi_{aa}=364.05(39)$ MHz. The theoretical values for ^{55}Mn are $\chi_{aa}=0.68$ MHz (eclipsed) and $\chi_{aa}=-5.87$ MHz (staggered) to be compared with the experimental value of $\chi_{aa}=-16.51(8)$ MHz. Thus the present Mn value of χ_{aa} of the staggered conformer is a significant improvement on the previous value[1] for the eclipsed conformer and the sign is now correct at both centers. The results for the Mn center are more sensitive to the basis set because the Mn electric field gradient (EFG) undergoes a sign change near the minimum-energy bond length.

The 784 basis set results given previously[1] showed that at both Mn and Re the quadrupole coupling decreases with increasing bond length, and that at each center this function could be closely fit to quadratic equations as a function of bond length.[1] However, basis sets and methodology are all important here. Comparisons of the EFGs from the BP86 and B3LYP functionals with the 874 basis set, at equilibrium and on the repulsive wall at Mn-Re 2.4 Å, show that the ratio EFG_{BB86}/EFG_{B3LYP} is 0.98 and ~0.76 for the Mn and Re centers, respectively. For the staggered conformer we fitted the EFGs at the Mn and Re centers as functions of Mn-Re distance using the function

$$V(r)=\frac{a_0+a_1(r-r_e)+a_2(r-r_e)^2+a_3(r-r_e)^3+a_4(r-r_e)^4}{1+b_2(r-r_e)^2+b_4(r-r_e)^4}, \tag{3}$$

where $r_e=3.113$ Å according to the Morse potential. The resulting fits are shown in Fig. 2. For a given vibrational state, an experiment would probe the quantum-mechanical average of the EFG, rather than its value at the equilibrium geometry. To assess this effect in the staggered conformer we computed the ground state quantum-mechanical average of the EFG, $\langle V\rangle$, assuming that the $Mn(CO)_5$ and $Re(CO)_5$ units form a heteronuclear pseudo-diatomic molecule. The necessary integral is,

$$\langle V\rangle=\int_{-\infty}^{\infty}\psi_0^*(r)V(r)\psi_0(r)dr, \tag{4}$$

where $\psi_0(r)$ is the normalized ground-state wavefunction of the harmonic oscillator and $V(r)$ is the EFG fitted as a function of Mn-Re distance, r. As we shall show in Sec. III E, the (experimental) vibrational mode most closely associated with the ''pseudo-diatomic'' Mn-Re stretch occurs at 89.9 cm^{-1}, or about 129 K. The reduced mass of the molecule was calculated by approximating it as a heteronuclear diatomic. Evaluating Eq. (4) using Simpson's rule integration, we find that for the Re center $\langle V\rangle=-0.3660$ a.u., which is to be compared with the fitted value of the EFG at $r=r_e$, which is $V(r_e)=-0.3672$ a.u. For the Mn center we find that $\langle V\rangle=+0.1290$ a.u. and $V(r_e)=+0.1286$ a.u. We therefore conclude that vibrational averaging in the ground state need not be taken into account. The vibrational energy level spacing is comparable to the thermal energy,[1] but we presume that quantum-mechanical averages in excited vibrational states will not deviate significantly from the corresponding equilibrium values. A full calculation of the thermal and quantum mechanical averages for the Morse potential is beyond the scope of this study.

We now turn to the dependence of the EFGs with the C-Re-Mn-C dihedral angle ϕ. In Fig. 3 we show the EFGs, V(Mn) and V(Re), for the Mn and Re centers, respectively, as functions of ϕ. It is clear that these are periodic functions of ϕ and so we have fitted the B3LYP results with functions analogous to that in Eq. (2), i.e.,

$$V(\phi)=\sum_{n=0} V_{4n}\cos(4n\phi). \tag{5}$$

The fits are included in Fig. 3, and the corresponding fit parameters and estimated errors are reported in Table III.

The temperature at which the microwave spectrum in Ref. 1 was measured is not accurately known. The sample was introduced to the apparatus at around 356 K, but because of the jet expansion the rotational temperature is likely to be in the range 10–20 K, while the intramolecular vibrational and torsional temperatures are probably considerably higher, possibly up to 100–150 K. Nonetheless, thermal averaging will necessarily lead to a change in the measured electric field gradient due to the statistical contributions from conformations deviating from the pure staggered geometry. To get a

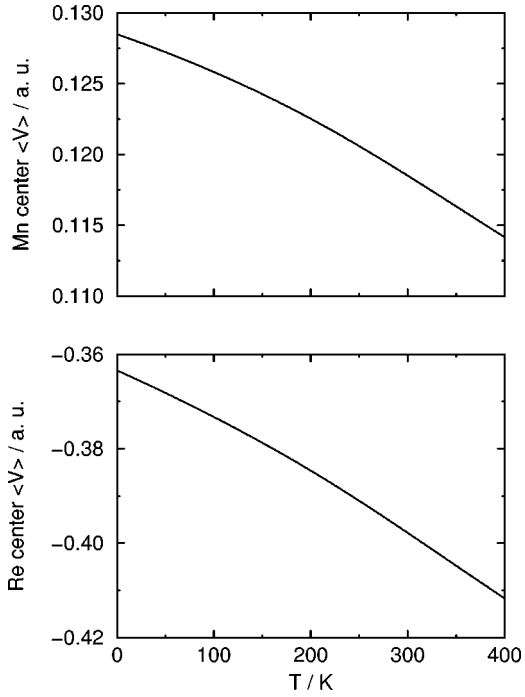

FIG. 4. Thermal averages of the electric field gradient $\langle V\rangle$ for the Mn center (top) and Re center (bottom) as function of temperature.

rough estimate of the effects of thermal averaging over the torsional motions we have computed the classical thermal average given by

$$\langle V\rangle = \frac{\int_0^{\pi/4} V(\phi)\exp[-E(\phi)/k_B T]d\phi}{\int_0^{\pi/4}\exp[-E(\phi)/k_B T]d\phi}, \tag{6}$$

where T is the temperature, k_B is Boltzmann's constant, and $E(\phi)$ and $V(\phi)$ are defined in Eqs. (2) and (5), respectively. Of course, this is only going to provide a very approximate description of the thermal average as we have ignored the quantization of torsional motions. The thermal torsional averages of the EFGs at the Mn and Re centers as functions of temperature are plotted in Fig. 4. To illustrate the effects of thermal variations, we consider three temperatures of $T=100$ K, 150 K, and 356 K. For the Mn center, the EFG averages are $\langle V\rangle_{100}=0.1258$ a.u., $\langle V\rangle_{150}=0.1243$ a.u., and $\langle V\rangle_{356}=0.1161$ a.u.; these numbers are to be compared with the (fitted) value at the equilibrium staggered ($\phi=\pi/4$) geometry, which is $V=0.1285$ a.u. The corresponding values for the Re center are $\langle V\rangle_{100}=-0.3733$ a.u., $\langle V\rangle_{150}=-0.3787$ a.u., and $\langle V\rangle_{356}=-0.4056$ a.u. which can be compared with the equilibrium value $V=-0.3634$ a.u. Thus the effects of thermal averaging give rise to only small variations, and are only around 10% even at 356 K. At the likely torsional temperatures produced by jet expansion, these variations are going to be even smaller.

E. Harmonic frequencies and intensities

We now discuss the harmonic frequencies for the staggered conformer, in the light of the extensive IR and Raman studies.[10–19] The effect of conformational change on intensities in IR/Raman studies at increased pressure has been discussed elsewhere[16] and is outside the scope of this investigation. Allowed bands are: A_1+E (IR) and $A_1+B_1+B_2+E$ (Raman),[14] however, the Raman spectrum has also been interpreted[12] as $A_1+``B_1''+E$, which allows additional coupling within the set of B_1 vibrations.[13,14] In the following discussion, we separate the B_1 and B_2 bands,[14] which have differing spatial motion.

The principal results of the present *ab initio* study of the harmonic vibration frequencies for Mn Re(CO)$_{10}$, using the B3LYP methodology with the 681 GTO basis set, are shown in Table IV, together with the IR and Raman intensities, polarization ratios, and principal motions of the atoms entered in order of declining importance; this basis set allowed the use of analytic derivative methods. The 784 basis set results, which use finite difference methods and hence are ''energy only'' determinations of IR vibration frequency, gave very similar results for band positions. LanL2DZ and LanL2MB bases did produce significant differences from the above, especially in the intensities.

The vibrational states have 44 distinct fundamentals being $13A_1+3A_2+6B_1+6B_2+16E$. These are conventionally defined as $\nu_1-\nu_{13}(A_1)$, $\nu_{14}-\nu_{16}(A_2)$, $\nu_{17}-\nu_{22}(B_1)$, $\nu_{23}-\nu_{28}(B_2)$, and $\nu_{29}-\nu_{44}(E)$, respectively. With the exception of the highest A_1 and E bands, the calculated A_1 bands are generally more intense in the infrared than E, while all of B_1, B_2, and A_2 have zero IR intensity. All three A_2 bands occur at low frequency and are also of zero intensity in the Raman spectrum. In many vibrational states the principal motion is not restricted to one $X(CO)_5$ equatorial or axial group. Thus, treating the two $X(CO)_5$ units as separate is only an approximation;[12,18] experimentally, internal rotation also increases the variety of CO interactions between the two main units.[18]

F. Comparison of harmonic frequencies with experimental data

Various wide-scan Raman and infrared spectra for Mn Re(CO)$_{10}$ are available,[16,18,19] but the temperatures, pressures,[16] and phases are not identical, leading to minor variations in observed frequencies; several coincidences of IR and Raman spectra occur, as well as bands occurring in only one of these spectra. Specific ^{13}CO labeling in the axial and equatorial positions has been used to assist assignment.[14] Many fundamentals have not yet been observed, and some observed bands may well be combination bands or overtones; this has led to controversy even in the ν_{CO} region, where differing assignments have been given for both band positions,[10–14] and for their symmetry assignments.[12,14,18] The principal experimental data, together with the present harmonic frequency sequence is shown in Table V. Direct comparison of the harmonic and anharmonic frequencies is only an approximation, but this has value in showing approximate positions of missing fundamentals and to suggest tentative assignments of the experimental spectrum on the basis of calculated intensity. We treat the three main observed IR/Raman frequency ranges separately.

The experimental band positions for the ν_{CO} region[12–14,18] agree probably within experimental errors, including phase effects (solutions and crystalline samples), for

TABLE IV. Harmonic frequencies (cm^{-1}), intensities, and atomic motion for the staggered conformer of Mn Re$(CO)_{10}$ compared with experiment.

Frequency 681 basis (cm^{-1})	Symmetry	IR intensity (km mol^{-1})	Raman activity ($Å^4$ amu^{-1})	Depolarization ratio, plane polarized	Depolarization ratio, unpolarized	Principal motion
2193.9	A_1	43.39	187.17	0.02	0.02	OC_{ax}(s), OC_{eq}(Re)
2111.2	A_1	1701.07	10.93	0.74	0.85	OC_{ax}(as), OC_{eq}(Mn)
2108.4	B_2	0.0	209.24	0.75	0.86	OC_{eq}(Re)
2087.8	E	2435.21	0.03	0.75	0.86	OC_{eq}(Re,Mn)
2071.1	A_1	77.22	350.00	0.66	0.79	OC_{ax}, OC_{eq}(Re)
2068.5	B_1	0.0	147.33	0.75	0.86	OC_{eq}(Mn)
2054.5	A_1	755.47	53.96	0.62	0.77	OC_{ax}, OC_{eq}(Mn,Re)
2047.2	E	136.61	13.37	0.75	0.86	OC_{eq}(Mn,Re)
683.6	A_1	269.02	0.94	0.57	0.72	C_{ax}Mn, C_{eq}Mn
672.0	E	99.67	0.00	0.75	0.86	C_{eq}Mn, C_{ax}Mn
599.1	A_1	316.48	0.55	0.38	0.55	C_{eq} Re, C_{ax} Re
584.4	E	53.22	1.36	0.75	0.86	C_{eq} Re
570.9	B_2	0.0	0.20	0.75	0.86	OC_{eq}Mn
568.1	E	5.94	0.42	0.75	0.86	OC_{ax}(Mn)OC_{eq}(Mn)
548.0	E	1.73	3.43	0.75	0.86	OC_{ax}(Re)OC_{eq}(Re)
507.2	B_1	0.0	0.10	0.75	0.86	OC_{eq} Re
500.7	B_2	0.0	0.89	0.75	0.86	OC_{eq} Re
492.0	A_1	0.56	13.58	0.0	0.0	OC_{ax}Mn, OC_{eq}Mn
484.7	A_1	1.57	0.46	0.15	0.25	OC_{ax} Re, OC_{eq} Re
479.1	B_1	0.0	1.36	0.75	0.86	OC_{eq}Mn
475.2	E	16.00	1.86	0.75	0.86	OC_{eq}Mn
447.0	A_1	1.42	20.75	0.01	0.01	OC_{ax} Re, OC_{eq} Re
437.7	B_2	0.0	2.87	0.75	0.86	OC_{eq} Re
427.3	E	0.55	0.09	0.75	0.86	OC_{ax}Mn, OC_{eq}Mn
413.1	B_1	0.0	3.00	0.75	0.86	OC_{eq}Mn
408.7	E	1.30	0.04	0.75	0.86	OC_{eq} Re, OC_{ax} Re
403.9	A_1	16.06	26.92	0.00	0.00	OC_{eq}Mn, OC_{ax} Re
381.5	A_2	0.0	0.0	0.0	0.0	OC_{eq}Mn
360.8	A_2	0.0	0.0	0.0	0.0	OC_{eq} Re
347.6	E	32.92	3.44	0.75	0.86	OC_{eq} Re
144.4	A_1	0.47	15.18	0.34	0.51	OC_{ax}Mn, OC_{eq}Mn
109.5	E	0.53	1.24	0.75	0.86	OC_{ax}Mn, OC_{eq}Mn
101.7	B_2	0.0	0.42	0.75	0.86	OC_{eq}Mn
97.6	E	0.03	0.02	0.75	0.86	OC_{eq} Re, OC_{ax} Re
94.3	A_1	0.31	12.90	0.16	0.28	Mn Re, OC_{eq}Mn
88.2	B_1	0.0	3.86	0.75	0.86	OC_{eq} Re
85.5	E	0.23	7.54	0.75	0.86	OC_{ax} Re, OC_{eq}Mn
82.8	A_1	2.93	0.24	0.15	0.25	OC_{eq} Re, OC_{ax} Re
72.3	B_1	0.0	2.15	0.75	0.86	OC_{eq}Mn
69.8	E	0.4	0.07	0.75	0.86	OC_{ax} Re, OC_{eq}Mn
62.9	B_2	0.0	0.59	0.75	0.86	OC_{eq} Re
56.4	E	~0.0	1.20	0.75	0.86	OC_{ax} Re Mn
53.8	E	0.05	0.93	0.75	0.86	OC_{ax}Mn Re
41.2	A_2	0.0	0.0	0.0	0.0	OC_{eq} Re, OC_{eq}Mn

all except two bands, namely 2030 cm^{-1} and 1993 cm^{-1}. Two bands occur in the Raman spectrum which are absent in the IR,[12,16] namely, 2038 and 1986 cm^{-1}, which have to be assigned as either B_1 and B_2 fundamentals or as overtones. The seven IR bands—$4A_1$ (ν_1 to ν_4) and $2E$ (ν_{29} and ν_{30})—shown by Sbrignadello, Battison, and Bor[14] (see their Figs. 2 and 3) especially, have similar relative intensities to our calculated sequence, but the agreement with other work[14,18,19] is also good. The calculated ν_{CO} region (Table IV) is complicated since three pairs of closely spaced bands occur with highly differing intensities. These pairs of bands do not follow a consistent order as the basis set increases; thus comparison with experiment becomes a question of where to place a shoulder on the wings of a strong band.

The present three highest fundamental assignments $A_1(\nu_1)$, $A_1(\nu_2)$, and $B_2(\nu_{23})$ are in agreement with previous experimental studies.[11,12,14] Only a single interchange of order occurs between the present ν_{CO} sequence and the sequence calculated with a previous force field.[11,12] With this exception, we feel that these assigned fundamentals are certain; the bands at 2044 and 2007 cm^{-1}, which seem well defined,[12,13,16] are probably overtones or combination bands.

The next region 550–700 cm^{-1} has five calculated and five observed bands (Raman and IR); these occur experimentally as a sharp doublet and singlet (both strong) followed by two very weak bands. Direct correlation of calculated and

TABLE V. Harmonic frequencies for the staggered conformer of Mn Re(CO)$_{10}$ compared with experimental IR and Raman spectra (cm^{-1}).

Calculated frequency 681 basis	Symmetry	Experiment			
		Infrared[a] C_6H_{12}	Infrared[b] C_6H_{12}	Raman[c]	Raman[d]
2193.9	A_1	2125.0 w	2124 w	2125 s	2126 m
2111.2	A_1	2054.5 m	2054 m		2117 vw
			2044 w		
2108.4	B_2		2031 vw	2035 m	2038 w
2087.8	E	2018.0 s	2017 vs		2025 vw
				2005 m	2009 m
2071.1	A_1	1999.5 vw	1998 w		2003 m
2068.5	B_1		1992 vw	1983 s	1986 s
2054.5	A_1	1979.5 m	1978 m		1965 vw
2047.2	E	1993.0 vw	1945 vw		
683.6	A_1		665 s	667	
672.0	E				
599.1	A_1		653 s	653	
584.4	E		598 s	590	588
570.9	B_2				
568.1	E		559 vw	556	562
548.0	E		540 vw	537	540
507.2	B_1				
500.7	B_2			503	
492.0	A_1		477 w	477	478
484.7	A_1				
479.1	B_1				
475.2	E			455	453
447.0	A_1			428	
437.7	B_2				
427.3	E				
413.1	B_1				
408.7	E		411 w	413	413
403.9	A_1		388 m	387	391
381.5	A_2				
360.8	A_2				
347.6	E		348 w	350	
144.4	A_1			155	157
109.5	E			111	111
101.7	B_2				
97.6	E				
94.3	A_1			94	95
88.2	B_1			84	
85.5	E				80
82.8	A_1				
72.3	B_1			68	68
69.8	E				
62.9	B_2			50	
56.4	E			34	36
53.8	E				
41.2	A_2			20	

[a]Reference 14.
[b]Reference 18.
[c]Reference 16.
[d]Reference 19.

experimental data would lead to the assignment 667+653 cm^{-1} (A_1+E) and 592 cm^{-1} (A_1). The middle frequency region from 400 to 550 cm^{-1} shows two IR bands[16,18] and three Raman bands[19] with rather differing intensity patterns. Almost all the IR intensity is in the band at 477 cm^{-1}, and this is close to the harmonic frequency of $\nu_{33}(E)$. The next range down to 350 cm^{-1} has three IR bands at 411, 385, and 348 cm^{-1}, with the middle one by far the most intense;[18] the Raman spectrum shows the same bands, but with most intensity in the highest band.[19] Only two of the calculated bands in this region have significant intensity, and we assign these (A_1+E) to 411 and 385 cm^{-1}, respectively.

The lowest frequency range shows[16,19] a group of at least eight Raman bands in the range 20–155 cm^{-1}; the calculated group of bands shows a maximum of intensity (four lines) near 120 cm^{-1}, with several nearly equally spaced lines to higher frequency. This region shows considerable difference under high pressure.[16] The 90 cm^{-1} calculated group of lines probably correlate with the observed broad maximum near 111 cm^{-1} and the isolated band at 155 cm^{-1} with the calculated line at 145 cm^{-1}.

IV. CONCLUSIONS

The present calculations of the potential energy surface demonstrate the relatively low barrier to internal rotation, and the ease of interconversion of the staggered and eclipsed conformers. There is only a very small barrier between the species for Mn-Re distances beyond ~5 Å. However, the staggered conformer always lies at lower energy, and the saddle point nature of the higher energy eclipsed conformer is demonstrated by a single imaginary harmonic frequency, which contrasts with the exclusively real set for the staggered conformer. The larger 874 basis set gives slightly better values for the Mn-Re equilibrium bond length when compared with the MW and crystallographic data, and the ^{55}Mn and ^{187}Re quadrupole coupling constants with this basis set are now both of correct sign, at equilibrium. Our previous result[1] gave ^{55}Mn coupling constant close to zero and of incorrect sign. The effects of both torsional thermal averaging over conformations and vibrational averaging over the Mn-Re stretching mode have been determined, but in both cases the effects are relatively small (<10%).

Detailed analysis of the experimental spectral Raman and IR data shows that the present calculations have considerable success both in terms of predicting groupings of harmonic frequencies in agreement with experimental bands and also predicting acceptable intensities within the three main ranges of absorption. However, at the very low frequency range, the present results are less secure.

ACKNOWLEDGMENTS

The authors gratefully acknowledge the National Science Foundation for providing financial support of this research. The authors thank the Edinburgh Parallel Computing Center for the provision of facilities on the Sun 'Sunfire 6800 SMP cluster', and to Dr. M. F. Guest, Dr. P. Sherwood, and Dr. H. J. J. van Dam, (CLRC Daresbury Laboratory) for help with the large basis set frequency calculations. The authors are grateful to Professor F. A. Cotton for suggesting the possibility of a low barrier to internal rotation for this complex.

[1] C. Tanjaroon, K. S. Keck, S. G. Kukolich, M. H. Palmer, and M. F. Guest, J. Chem. Phys. **120**, 4715 (2004).
[2] GAMESS-UK (V6.3): M. Dupuis, D. Spangler, and J. Wendoloski, NRCC Software Catalog, Vol. 1, Program No. QG01 (GAMESS), 1980.
[3] M. F. Guest, J. Kendrick, J. H. van Lenthe, K. Schoeffel, and P. Sherwood, 'GAMESS-UK: Users Guide and Reference Manual', Version 5, Computing for Science (CFS) Ltd. (Daresbury Laboratory, Warrington, UK, 1994).
[4] G. A. Junk and H. J. Svec, J. Chem. Soc. A 2102 (1970).
[5] A. L. Rheingold, W. K. Meckstroth, and D. P. Ridge, Inorg. Chem. **25**, 3706 (1986).
[6] M. R. Churchill and R. Bau, Inorg. Chem. **6**, 2086 (1967).
[7] C. P. Casey, C. R. Cyr, R. L. Anderson, and D. F. Marten, J. Am. Chem. Soc. **97**, 3053 (1975).
[8] O. Orama, U. Schubert, F. R. Kreissl, E. O. Fischer, and Z. Naturforch, Z. Naturforsch. B **35**, 82 (1980).
[9] F. A. Cotton and D. C. Richardson, Inorg. Chem. **5**, 1851 (1966).
[10] H. M. Gager, J. Lewis, and M. J. Ware, J. Chem. Soc., Chem. Commun. 616 (1966).
[11] G. O. Evans, W. T. Wozniak, and R. K. Sheline, Inorg. Chem. **9**, 979 (1970).
[12] W. T. Wozniak, G. O. Evans, and R. K. Sheline, J. Inorg. Nucl. Chem. **37**, 105 (1975).
[13] G. O. Evans, W. T. Wozniak, and R. K. Sheline, Inorg. Chim. Acta **14**, L53 (1975).
[14] G. Sbrignadello, G. Battison, and G. Bor, Inorg. Chim. Acta **14**, 69 (1975).
[15] R. A. Levenson and H. B. Gray, J. Am. Chem. Soc. **97**, 6042 (1975).
[16] D. M. Adams and I. O. C. Ekejuiba, J. Chem. Phys. **78**, 5408 (1983).
[17] S. Firth, P. M. Hodges, M. Poliakoff, and J. J. Turner, Inorg. Chem. **25**, 4608 (1986).
[18] N. Flitcroft, D. K. Huggins, and H. D. Kaesz, Inorg. Chem. **3**, 1123 (1964).
[19] C. O. Quicksall and T. G. Spiro, Inorg. Chem. **8**, 2363 (1969).